Article Title	Studies on Catalytic Pyrolysis of Empty Fruit Bunch (EFB) using Taguchi’s L9 Orthogonal Array

Authors

Name	**Title / Contact Details**
CHAN YI HERNG	MSc Student Chemical Engineering Department, Universiti Teknologi PETRONAS, Bandar Seri Iskandar, 31750 Tronoh, Perak, Malaysia. Email: kelvinyiherng@gmail.com
DANG KHANH VI	MSc Student Chemical Engineering Department, Universiti Teknologi PETRONAS, Bandar Seri Iskandar, 31750 Tronoh, Perak, Malaysia. Email: dangkhanhvi@gmail.com
SUZANA YUSUP* (Corresponding author)	PhD (University of Bradford, UK) Associate Professor Chemical Engineering Department, Universiti Teknologi PETRONAS, Bandar Seri Iskandar, 31750 Tronoh, Perak, Malaysia. Phone: + 6053687642, Fax: +6053688204, Email: drsuzana_yusuf@petronas.com.my
LIM MOOK TZENG	PhD (University of Canterbury, NZ) Postdoctoral Researcher, Green Technology, Universiti Teknologi PETRONAS, Bandar Seri Iskandar, 31750 Tronoh, Perak, Malaysia. Phone: + 6053688208, Email: lim.mooktzeng@petronas.com.my
ASNA MOHD ZAIN	Lecturer Chemical Engineering Department, Universiti Teknologi PETRONAS, Bandar Seri Iskandar, 31750 Tronoh, Perak, Malaysia Phone: +6053687614, Email: asnamz@petronas.com.my
YOSHIMITSU UEMURA	Head, Center for Biofuel and Biochemical Research Mitsubishi Chair in Green Technology Chemical Engineering Department, Universiti Teknologi PETRONAS, Bandar Seri Iskandar, 31750 Tronoh, Perak, Malaysia Phone: +6053687644, Email: yoshimitsu_uemura@petronas.com.my

Studies on Catalytic Pyrolysis of Empty Fruit Bunch (EFB) using Taguchi's L9 Orthogonal Array

Y. H. Chan, D. K. Vi, S. Yusup[*], M. T. Lim, A. M. Zain and Y. Uemura

Biomass Processing Lab, Centre for Biofuel and Biochemical, Green Technology,
Mission Oriented Research, Chemical Engineering Department,
UNIVERSITI TEKNOLOGI PETRONAS, Bandar Seri Iskandar, 31750 Tronoh, Perak, Malaysia.
*Corresponding author. *E-mail address:* drsuzana_yusuf@petronas.com.my

ABSTRACT

This paper investigates the effects of four reaction parameters that include type of catalyst, catalyst loading, reaction temperature and nitrogen gas flowrate on the liquid (bio-oil) yield from the catalytic pyrolysis of Empty Fruit Bunch (EFB). The experimental design is based on Taguchi's L9 Orthogonal Array in which the reaction parameters are varied at three levels. The maximum liquid yield is predicted based on systematic experimental runs, and is found to be at 5 wt-% of H-Y catalyst, 500°C and at nitrogen flowrate of 100 ml min^{-1}. The predicted maximum liquid yield is validated with an experimental run at the corresponding predicted conditions. The bio-oil produced at the optimum reaction condition is characterized and compared with known bio-oil standards in the literature.

Keywords: catalytic pyrolysis, empty fruit bunch, Taguchi's L9 Orthogonal Array, bio-oil.

---

1. INTRODUCTION

The fluctuating prices of fossil fuels and the detrimental effects of fossil fuel utilization have increased the importance of renewable energy resources. Among all these alternative renewable energy sources, biomass is considered to be one of the most attractive options, because unlike other renewable sources of energy (i.e. solar, wind), biomass can be converted to liquid, solid and gaseous fuels, [1] and a range of specialty chemicals. Furthermore, as pointed out by Chang et al. (2008), biomass utilization is carbon neutral as it does not emit additional carbon dioxide and carbon monoxide (greenhouse gases), NO_x and SO_x into the atmosphere, reducing the usage of fossil fuels as well as mitigating the impact on the environment. [2]

Biomass can be converted to energy via two pathways; biological (fermentation and anaerobic digestion) and thermochemical (gasification, liquefaction and pyrolysis) processes. [3] Thermochemical conversion via pyrolysis is a promising process as it produces mainly liquid bio-oil, along with solid char and gas as valuable byproducts. Bio-oil can substitute fuel oil or diesel in many static applications, such as boilers, furnaces, engines and turbines to generate electricity. [4] Besides, it can be upgraded to extract various chemicals such as acetic acid, food flavorings, preservatives, adhesives, hydrogen, resins and sugars.

As pyrolysis can be a slow process which requires several minutes, the reaction can be improved and enhanced by the introduction of catalyst. Catalysts facilitate the cracking of carbon-carbon bonds and de-oxygenation reaction, producing bio-oil that is lower in oxygenates, has a higher calorific value and better hydrocarbon distribution. Hence the quality and stability of bio-oil is improved, making the handling, upgrading and transporting of bio-oils easier in addition to reduction of costs of downstream upgrading processes. [3,5-8]

Various parameters affect the pyrolysis process, which include the temperature and heating rate of the reactor, the properties of different biomass and catalysts, the water content, the design of the reactor and the catalyst loading. Investigating the effect of the parameters individually is costly and time consuming. Thus, to reduce the number of experiment, Taguchi's Orthogonal Array can be used to perform a number of representative experiments. Taguchi's Orthogonal Array is utilized in various fields, such as the medical industry, pollution control, therapeutic and pharmaceutical industries. [9-12] Not many investigations have utilized Taguchi's Orthogonal Array to determine the optimum reaction parameters for bio-oil production.[13]

In this study, the catalytic pyrolysis of empty fruit bunch (EFB) is investigated. EFB is one of the solid waste from palm oil industry. [14] The effects of catalyst type, catalyst loading, reaction temperature and nitrogen flowrate on the liquid (bio-oil) yield from the pyrolysis process is predicted and optimized using the Taguchi's L9 Orthogonal Array method. The optimum reaction condition that produces the maximum liquid yield is predicted and compared with the experimental results. The characteristics of the bio-oil obtained at the optimum reaction condition are characterized and compared with known bio-oil standards.

2. MATERIALS AND METHODS

2.1 Materials

Fresh EFBs are obtained from *FELCRA Nasaruddin Oil Palm Mill, Bota, Perak, Malaysia*. These EFBs are washed and dried in an oven at 80 °C for three days. The dried EFB are manually chopped and cut into smaller pieces. They are then washed with water to remove the sand and dust particles. Then, they are dried again in the oven at 80 °C. The particle size of the dried EFB is reduced with a FRITSCH Cutting Mill and is sieved to a particle size of smaller than 500 µm. The EFB is dried in the oven at 105 °C for at least 24 hours before being used in the catalytic pyrolysis experiments. Chemical composition of the EFB and higher heating value (HHV) are summarized in Table 1. Both properties are determined using a LECO 932 CHNS Analyzer and the IKA C5000 Bomb Calorimeter respectively.

Table 1: Chemical composition of EFB

Properties	Measured value
Carbon /mf wt-%	46.83
Hydrogen /mf wt-%	6.277
Nitrogen /mf wt-%	0.664
Sulfur /mf wt-%	0.237
Oxygen (by difference) /mf wt-%	45.992
HHV /MJ kg^{-1}	19.643

The zeolite catalysts used in this study are obtained from Zeolyst International. Their properties are summarized in Table 2.

Table 2: Properties of zeolite catalysts

Type of catalyst	SiO_2/Al_2O_3	Surface Area / $m^2\ g^{-1}$	Pore Size / Å [15]
H-ZSM-5	30	400	5.1×5.5 5.3×5.6
H-Beta	25	680	6.6×6.7 5.6×5.6
H-Y	30	780	7.4×7.4

2.2 Experimental Procedure and Plan

The experimental runs with four parameters are determined using Design Expert, a statistical software which incorporates Taguchi's L9 Orthogonal Array Method. The software determines nine significant experimental runs instead of 81 runs in the case of 4 reaction parameters, with 3 levels each; $3^4 = 81$. The four reaction parameters or factors in this study are: the type of catalysts, catalyst loading, the reaction temperature and the nitrogen flowrate. The levels of each factor are summarized in Table 3 and the significant nine runs determined from the Taguchi's Orthogonal Array Method are summarized in Table 4. Based on the liquid yield data obtained from the nine runs in Table 4, the liquid yield for the other combination of factors is also predicted from the Taguchi's L9 Orthogonal Array. From the predicted results, the conditions for maximum liquid yield are obtained. An experimental run is performed at the predicted condition to validate the predicted liquid yield. The characteristics of bio-oil that is produced at the optimum reaction condition are also determined.

Table 3: Reaction parameters and their levels

Reaction Parameters	Level 1	Level 2	Level 3
Factor A: Type of catalyst	H-Beta	H-Y	H-ZSM-5
Factor B: Catalyst Loading /wt-%	1	5	12
Factor C: Reaction Temperature /°C	450	500	550
Factor D: Nitrogen Flowrate /ml min^{-1}	100	300	500

Table 4: Experimental runs and corresponding parameters determined from Taguchi's L9 Orthogonal Array

Run	Type of catalyst	Catalyst Loading /wt- %	Reaction Temperature /°C	Nitrogen Flowrate /ml min^{-1}
1	H-Y	5	450	500
2	H-ZSM-5	1	450	100
3	H-ZSM-5	12	550	500
4	H-Beta	5	550	100
5	H-ZSM-5	5	500	300
6	H-Beta	1	500	500
7	H-Beta	12	450	300
8	H-Y	12	500	100
9	H-Y	1	550	300

The signal-to-noise (S/N) ratio, which indicates the effect of each variable on the liquid yield, is calculated using the-higher-the-better criteria for each factor since a higher liquid yield from the pyrolysis process is needed. The equation for the calculation of S/N ratio is shown in equation (1):

$$(S/N) = -10\log\left(\frac{1}{r}\sum_{i=1}^{r}\frac{1}{y_i^2}\right) \qquad (1)$$

where r is the number of tests in a trial, y_i is the experimental response at ith repetition. In order to examine the significance of each individual factor on the liquid yield, the average S/N value for each factor f at level j is computed for each factor and level, as shown in equation (2): [16-17]

$$S / N = \frac{\text{Sum of S/N values for factor } i \text{ at each level } j}{3} \qquad (2)$$

The range of S/N ratio values (Δ) is calculated for each factor and a larger range signifies a higher influence on the liquid yield.

2.3 Equipment

The reactor used in this study is a tube furnace reactor with an inner diameter of 25 mm and a length of 340 mm, as shown in Figure 1.

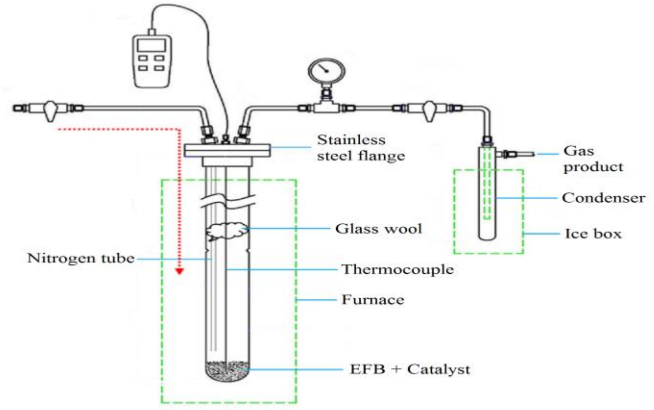

Figure 1: Tube Furnace (Semi-Batch) Reactor (PI2013001664)

In each experimental run, 15 g of dried EFB are mixed with catalysts into a borosilicate glass tube, which is inserted into the tube furnace. The tube furnace is equipped with heating elements rated at 1.5 kW, thus the temperature can be varied accordingly. Nitrogen gas is used to flush out oxygen in the reactor. Then, the temperature of the reactor and the nitrogen flowrate are varied according to the values in Table 4. The heating rate of the furnace is fixed at 20 °C min^{-1}. Gas is produced from pyrolysis reaction in the system, and is flushed out by nitrogen and passed through an ice bath, where part of the gases is condensed as bio-oil. The weight of the condensed bio-oil is determined by measuring the weight of the condenser before and after the experiment. The liquid yield from the pyrolysis process is calculated from the amount of bio-oil produced based on the original biomass used, according to the following equation (3).

$$\text{Liquid or bio-oil yield} = \frac{\text{Weight of bio-oil}}{\text{Weight of biomass}} \times 100\% \qquad (3)$$

2.4 Characterization of bio-oil

The bio-oil produced is tested for water content with Metrohm 870 Karl Fischer Titrino Plus. The density, pH value, viscosity and heating value are measured using Anton Paar Density Meter DMA 4500 M, EUTECH Instruments pH 510 pH/mV/°C Meter, Brookfield CAP 2000+ Viscometer and IKA C5000 Bomb Calorimeter respectively. Ultimate analysis of the bio-oil is also performed using LECO CHNS Analyzer 932 to determine its elemental content.

3. RESULTS AND DISCUSSION

3.1 Predicted maximum liquid yield and effect of individual factors on liquid yield

The experimental results for the nine runs are shown in Table 5 and are used to predict the optimum liquid. Table 6 shows the predicted liquid yield for other combination of factors and levels and the liquid yield from the nine experimental runs. Figure 2 and 3 show the interaction effects of catalyst type, catalyst loading, temperature and nitrogen flowrate on the experimental liquid yield. From these two figures, it can be seen that the maximum liquid yield of 45.98 wt-% is obtained using 5 wt-% of H-Y catalyst loading, temperature of 500 °C and at nitrogen flowrate of 100 ml min^{-1}.

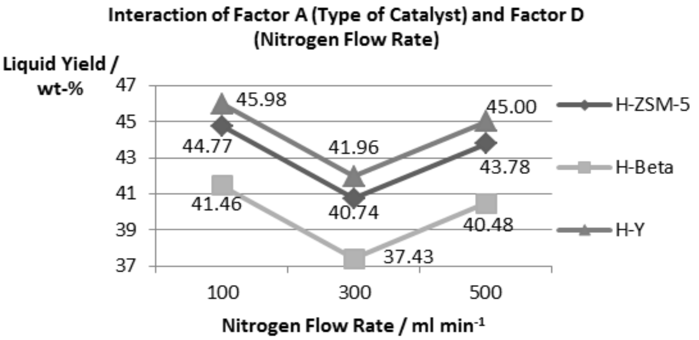

Figure 2: Interactive effects of catalysts type and nitrogen flowrate on the liquid yield for 5 wt-% of catalyst loading at reaction temperature of 500 °C.

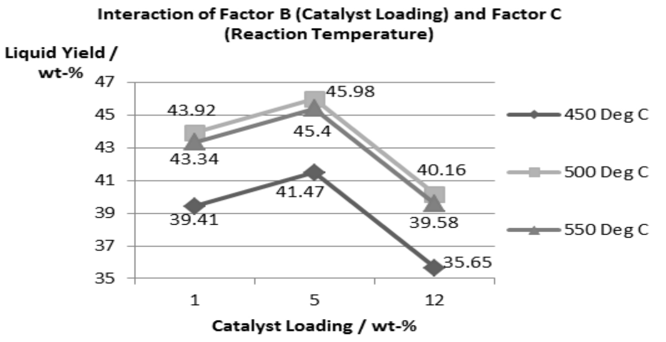

Figure 3: Interactive effects of catalyst loading and temperature on the liquid yield for H-Y catalyst at 100 ml min^{-1} of nitrogen flow.

An experimental run at the predicted optimum conditions is performed to validate the liquid yield from the predicted data.

From the experimental run, the liquid yield is 44.05 wt-%, which is very close to the predicted liquid yield.

Table 5: Experimental liquid yield from pyrolysis reactor

Run	Experimental liquid yield /wt-%	(S/N) ratio
1	40.49	32.15
2	38.19	31.64
3	37.38	31.45
4	40.88	32.23
5	40.74	32.20
6	38.41	31.69
7	27.10	28.66
8	40.16	32.08
9	39.31	31.89

From Table 7, the range of S/N ratio is the highest referring to catalyst loading, followed by type of catalyst, reaction temperature and nitrogen flowrate. This means that the catalyst loading has the highest influence on the liquid yield, because a change in the factor causes a larger impact on the liquid yield, resulting in a larger S/N ratio range (Δ).

Table 7: S/N ratio values for each factor and level

Level	Type of catalyst	Catalyst Loading	Reaction Temperature	Nitrogen Flowrate
1	30.86	31.74	30.82	31.98
2	32.04	32.19	31.99	30.92
3	31.76	30.73	31.86	31.76
Range (Δ)	1.18	1.46	1.17	1.06
Rank	2	1	3	4

3.1.1 Effect of catalyst type on liquid yield

The difference in liquid yield using three catalysts can be explained in terms of its acidity (SiO_2/Al_2O_3 ratio), surface area and the pore size of the catalysts. Catalyst with higher acidity which has lower value of SiO_2/Al_2O_3 ratio will produce less liquid bio-oil because the high acidity of the catalyst promotes higher decomposition and cracking of pyrolysis vapor. [18] This agrees well with the results obtained; H-β gives the lowest liquid yield as it has the highest acidity at a SiO_2/Al_2O_3 ratio of 25, compared to H-ZSM-5 and H-Y, both with lower acidity at SiO_2/Al_2O_3 ratios of 30 as shown in Table 2. The H-Y catalyst has a larger surface area of 780 $m^2 g^{-1}$ compared to that of H-ZSM-5 (400 $m^2 g^{-1}$), which allows more active sites of the catalyst to be exposed for reactions, hence giving higher liquid yield. On the other hand, larger pore size of H-Y catalyst (7.4 × 7.4 Å) compared to that of H-ZSM-5 (5.1×5.5 5.3×5.6 Å) has reduced the liquid yield. As reported by Park et al. (2011) and Du et al. (2013), catalyst with larger pore size tends to have higher coke and tar formation. [19-20] As a result, it causes higher degree of catalyst deactivation, leading to decreased liquid yield. Thus, the liquid yield produced using H-Y catalyst is slightly higher than that of H-ZSM-5 as in Fig. 2, which is similar to the findings reported in the literature. [15]

3.1.2 Effect of nitrogen flowrate on liquid yield

The liquid yield is observed to vary less significantly with increasing nitrogen flowrate as compared to the other three factors as shown in Fig. 2, and this is synonymous with the S/N ratios in Table 7, where the S/N ratio for the nitrogen flowrate is the least compared to other three factors. The change in nitrogen flowrate causes about 4.03 wt-% of variation in the liquid yield compared to about 5.82 wt-% of variation for effect of catalyst loading, 4.52 wt-% of variation for the effect of type of catalyst and 4.51 wt-% of variation for the effect of reaction temperature. The flowrate of sweeping gas might affect the liquid yield in which higher nitrogen flowrate decreases the vapor residence times. These residence times in the literature were reported to be in the range of 40 s to 560 s, depending on the type of reactor, [7, 21-22] while the residence time in this study is approximately 80, 133 and 400 s for nitrogen flowrate of 500, 300 and 100 ml min^{-1} respectively. Higher nitrogen flowrate removes pyrolysis vapor from the reaction zone rapidly and hence, prevents secondary reactions of the vapor thus increasing the liquid yield. On the other hand, high nitrogen flowrate might also cause insufficient quenching of pyrolysis vapor that might decrease the liquid yield. [7,21] Hence, the determination of optimum sweeping gas flowrate in the pyrolysis of biomass should be given further consideration and investigation.

3.1.3 Effect of catalyst loading on liquid yield

Figure 3 shows that as the catalyst loading increases from 1 wt-% to 5 wt-%, the liquid yield increased. However as the catalyst loading increases from 5 wt-% to 12 wt-%, the liquid yield decreased. The increase in liquid yield with the catalyst is due to an increase of the rate of decomposition and cracking in the pyrolysis reaction.[23] However, further increase in catalyst loading could cause secondary reactions which convert the pyrolysis vapors into non-condensable gases, hence decreased the amount of bio-oil produced. This trend is consistent with other researchers' works [3,5-7] which showed that the introduction of catalyst in catalytic pyrolysis decreased the amount of organic yield (bio-oil) and increased the amount of gas yield, water content and polyaromatic hydrocarbons (PAHs). French et al. (2010) pointed out that the oxygenated compounds in the bio-oil undergo dehydration, decarboxylation, cracking, aromatization, alkylation, condensation and polymerization with de-oxygenation simultaneously. [18] At lower temperatures, oxygen in the biomass is removed as H_2O (dehydration) whereas at higher temperatures, oxygen is removed as CO_2 (decarboxylation) and CO (decarbonylation). [24-25] The second reason for the low yield of bio-oil is because of rapid deactivation of catalyst which caused catalyst coking. [6-7,25-27]

Table 6: Liquid Yield Based on Taguchi's L9 Orthogonal Array's Prediction. The liquid yield from the nine experimental runs are marked with ' * ', the other yields are predicted from Taguchi's method.

No.	Factor A	Factor B	Factor C	Factor D	Yield /wt-%	Note
1	H-Y	1	450	100	39.41	
2	H-Y	1	450	300	35.38	
3	H-Y	1	450	500	38.42	
4	H-Y	1	500	100	43.92	
5	H-Y	1	500	300	39.89	
6	H-Y	1	500	500	42.93	
7	H-Y	1	550	100	43.34	
8	H-Y	1	550	300	39.31	*
9	H-Y	1	550	500	42.35	
10	H-Y	5	450	100	41.47	
11	H-Y	5	450	300	37.45	
12	H-Y	5	450	500	40.49	*
13	H-Y	5	500	100	45.98	
14	H-Y	5	500	300	41.96	
15	H-Y	5	500	500	45.00	
16	H-Y	5	550	100	45.40	
17	H-Y	5	550	300	41.38	
18	H-Y	5	550	500	44.42	
19	H-Y	12	450	100	35.65	
20	H-Y	12	450	300	31.62	
21	H-Y	12	450	500	34.67	
22	H-Y	12	500	100	40.16	*
23	H-Y	12	500	300	36.13	
24	H-Y	12	500	500	39.18	
25	H-Y	12	550	100	39.58	
26	H-Y	12	550	300	35.55	
27	H-Y	12	550	500	38.60	
28	H-ZSM-5	1	450	100	38.19	*
29	H-ZSM-5	1	450	300	34.16	
30	H-ZSM-5	1	450	500	37.21	
31	H-ZSM-5	1	500	100	42.7	
32	H-ZSM-5	1	500	300	38.67	
33	H-ZSM-5	1	500	500	41.72	
34	H-ZSM-5	1	550	100	42.12	
35	H-ZSM-5	1	550	300	38.09	
36	H-ZSM-5	1	550	500	41.14	
37	H-ZSM-5	5	450	100	40.26	
38	H-ZSM-5	5	450	300	36.23	
39	H-ZSM-5	5	450	500	39.27	
40	H-ZSM-5	5	500	100	44.77	
41	H-ZSM-5	5	500	300	40.74	*
42	H-ZSM-5	5	500	500	43.78	
43	H-ZSM-5	5	550	100	44.19	
44	H-ZSM-5	5	550	300	40.16	
45	H-ZSM-5	5	550	500	43.20	
46	H-ZSM-5	12	450	100	34.43	
47	H-ZSM-5	12	450	300	30.41	
48	H-ZSM-5	12	450	500	33.45	
49	H-ZSM-5	12	500	100	38.94	
50	H-ZSM-5	12	500	300	34.92	
51	H-ZSM-5	12	500	500	37.96	
52	H-ZSM-5	12	550	100	38.36	
53	H-ZSM-5	12	550	300	34.34	
54	H-ZSM-5	12	550	500	37.38	*
55	H-Beta	1	450	100	34.88	
56	H-Beta	1	450	300	30.86	
57	H-Beta	1	450	500	33.90	
58	H-Beta	1	500	100	39.39	
59	H-Beta	1	500	300	35.37	
60	H-Beta	1	500	500	38.41	*
61	H-Beta	1	550	100	38.81	
62	H-Beta	1	550	300	34.79	
63	H-Beta	1	550	500	37.83	
64	H-Beta	5	450	100	36.95	
65	H-Beta	5	450	300	32.92	
66	H-Beta	5	450	500	35.97	
67	H-Beta	5	500	100	41.46	
68	H-Beta	5	500	300	37.43	
69	H-Beta	5	500	500	40.48	
70	H-Beta	5	550	100	40.88	*
71	H-Beta	5	550	300	36.85	
72	H-Beta	5	550	500	39.90	
73	H-Beta	12	450	100	31.13	
74	H-Beta	12	450	300	27.10	*
75	H-Beta	12	450	500	30.14	
76	H-Beta	12	500	100	35.64	
77	H-Beta	12	500	300	31.61	
78	H-Beta	12	500	500	34.65	
79	H-Beta	12	550	100	35.06	
80	H-Beta	12	550	300	31.03	
81	H-Beta	12	550	500	34.07	

3.1.4 Effect of reaction temperature on liquid yield

Figure 3 shows that as the temperature increases, the rate of reaction also increases, hence increasing the liquid yield. [7] There is a decrease in liquid yield when the temperature increased from 500 °C to 550 °C due to the secondary decomposition reaction of the liquid fraction of volatiles that produced incondensable pyrolysis vapor. Similar trends are also reported in other findings. [4,7,28-31]

3.2 Bio-oil characteristics

The properties of the bio-oil produced at optimum condition are measured and summarized in Table 8. The range of water content of bio-oil obtained from literature is found to vary from 8 to 75 %. This large range of the water content is due to the difference in the types of pyrolysis reaction, various feedstocks and the mode of operation of reactors. Catalytic pyrolysis reactions generally produce bio-oil with higher water content compared to that of non-catalytic pyrolysis. This is because the acidic catalyst improves the de-oxygenation of bio-oil and dehydration reaction, hence forming a higher amount of water at the expense of organic oil. [4,6,18,32] This can be shown when the water content of bio-oil produced in this study (50 wt-%) is higher than that of non-catalytic pyrolysis, [4,31-32] but is comparable to those of catalytic pyrolysis. [28-30,32]

The ultimate analysis of the bio-oil produced in this study is also shown in Table 8, and it can be seen that the bio-oil is similar in composition to that of wood derived bio-oil. [28-30]

As the bio-oil produced in this study has a higher water content (50%), the HHV measured is slightly lower compared to the values measured in the literature. [4,31-32]

Table 8: Properties of bio-oil produced at optimum reaction condition and comparison with existing literatures

References	This work	[4]	[28-30]	[7]	[33]	[31]	[32]
Water Content /wt-%	50	25	7.90-64.01 (depending on the feedstock)	…	…	20-30	25-75 (depending on the type of pyrolysis)
pH	2.69	2.5	…	…	3.0-3.4	2.5	2.5
Viscosity (at 40 °C) / cP	45.47	40-100	…	…	…	30-200	40-1000
Density /g cm^{-3}	1.0699 (at 20°C)	…	…	…	0.832-1.170 (at 30 °C)	…	…
Ultimate Analysis / %							
Carbon	25.33	56	32-48	77.62	…	56.4	50-58
Hydrogen	9.317	6	7-8.5	12.15	…	6.2	5.5-7.0
Nitrogen	0.317	0-0.1	<0.4	5.33	…	0.2	<0.2
Sulfur	0.451	…	<0.05	0	…	<0.01	…
Oxygen (by difference)	64.585	38	44-60	4.9	…	37.1	35-42
HHV /MJ kg^{-1}	10.425	17	…	42.91	…	17 (25 % moisture)	16-19 (15-30 % moisture)

4. CONCLUSION

The influence of four reaction parameters; type of catalyst, catalyst loading, reaction temperature and nitrogen gas flowrate on the liquid (bio-oil) yield is investigated and studied. Catalyst loading has the most significant influence, followed by type of catalyst, reaction temperature and nitrogen gas flowrate based on the computation of signal-to-noise (S/N) ratio using the-higher-the-better criteria for each factor. Besides, the ranking is also consistent with the variation of liquid yield brought about by the change in the levels of a certain factor (catalyst loadings caused a variation of 5.82 wt-% in liquid yield, followed by type of catalyst which caused a variation of 4.52 wt-% in liquid yield, reaction temperature which caused a variation of 4.51 wt-% in liquid yield and nitrogen gas flowrate which caused a variation of 4.03 wt-% in liquid yield).

In the design of the experiment, Taguchi L9 Orthogonal Array Method is used to determine and predict the optimum reaction condition based on nine runs. The predicted maximum liquid yield is 45.98 wt-%, using 5 wt-% of H-Y catalyst at temperature of 500 °C and nitrogen flowrate of 100 ml min^{-1}. This condition is validated based on experimental result, giving a yield of 44.05 wt-%, which is close to the predicted yield.

The properties of the bio-oil produced at optimum condition are consistent with the known standards of bio-oils. As catalyst promotes dehydration reaction, the bio-oil produced in this work has higher water content. Other physical properties such as pH value, viscosity, higher heating value and density are consistent with the standards obtained from other existing literatures.

Acknowledgement

The authors would like to express their greatest gratitude to UNIVERSITI TEKNOLOGI PETRONAS for the financial and technical support.

References

[1] M.H. Nilsen, E. Antonakou, A. Bouzga, A. Lappas, K. Mathisen, M. Stöcker: 'Investigation of the effect of metal sites in the Me-Al-MCM-41 (Me = Fe, Cu or Zn) on the catalytic behavior during the pyrolysis of wooden based biomass', *Microporous and Mesoporous Materials*, 2007, **105**, 189-203.

[2] W. Chang, H. Qinglan, L. Dingqiang, J. Qingzhu, L. Guiju, X. Bo: 'Production of Light Aromatic Hydrocarbon from Biomass by Catalytic Pyrolysis', *Chinese Journal of Catalysis*, 2008, **29 (9)**, 907-912.

[3] W. Denghui, X. Rui, Z. Huiyan, H. Guangying: 'Comparison of catalytic pyrolysis of biomass with MCM-41 and CaO catalysts by using TGA-FTIR analysis', *Journal of Analytical and Applied Pyrolysis*, 2010, **89**, 171-177.

[4] M. Crocker (ed.): 'Thermochemical Conversion of Biomass to Liquid Fuels and Chemicals'; 2010, United Kingdom, The Royal Society of Chemistry.

[5] A. Aho, N. Kumar, K. Eränen, T. Salmi, M. Hupa, D.Y. Murzin: 'Catalytic Pyrolysis of Biomass In A Fluidized Bed Reactor: Influence of the acidity of H-Beta Zeolite', *Trans IChemE, Part B, Process Safety and Environmental Protection*, 2007, **85(B5)**, 473-480, doi: 10.1205/psep07012

[6] A. Aho, N. Kumar, K. Eränen, T. Salmi, M. Hupa, D. Yu. Murzin: 'Catalytic pyrolysis of woody biomass in a fluidized bed reactor: Influence of the zeolite structure', *Fuel*, 2008, **87**, 2493-2501.

[7] E. Pütün: 'Catalytic Pyrolysis of biomass: Effects of pyrolysis temperature, sweeping gas flow rate and MgO catalyst', *Energy*, 2010, **35**, 2761-2766.

[8] S. Thangalazhy-Gopakumar, S. Adhikari, R.B. Gupta, M. Tu, S. Taylor: 'Production of hydrocarbon fuels from biomass using catalytic pyrolysis under helium and hydrogen environments', *Bioresource Technology*, 2011, **102**, 6742-6749.

[9] T.T. Ajaal and R.W. Smith: 'Employing the Taguchi method in optimizing the scaffold production process for artificial bone grafts', *Journal of Materials Processing Technology*, 2009, **209**, 1521-1532.

[10] M.P. Elizalde-González and L.E. García-Díaz: 'Application of a Taguchi L_{16} orthogonal array for optimizing the removal of Acid Orange 8 using carbon with low surface area', *Chemical Engineering Journal*, 2010, **163**, 55-61.

[11] S. Saravanan, G. Nagarajan, S. Sampath: 'Application of Taguchi's Orthogonal Array in Multi Response Optimization of NO_x Emission of Crude Rice Bran Oil Methyl Ester Blend as a CI Engine Fuel', *Open Journal of Optimization*, 2012, **1**, 25-33.

[12] D. Shravani, P.K. Lakshmi, J. Balasubramaniam: 'Preparation and Optimization of various parameters of enteric coated pellets using the Taguchi L9 orthogonal array design anf their characterization', *Acta Pharmaceutica Sinica B*, 2011, **1**(1), 56-63.

[13] C. Yen-Chang, P. Yung-Ning, H. Kuo-Huang: 'Process Optimization of Fast Pyrolysis Reactor for Converting Forestry Wastes into Bio-oil with the Taguchi Method', *Procedia Environmental Sciences*, 2011, **10**, 1719-1725.

[14] R. Omar, A. Idris, R. Yunus, K. Khalid, M.I. Aida Isma: 'Characterization of empty fruit bunch for microwave-assisted pyrolysis', *Fuel*, 2011, **90**, 1536-1544.

[15] H. Ben and A.J. Ragauskas: 'One step thermal conversion of lignin to gasoline range liquid products by using zeolites as additives', *RSC Advances*, 2012, **2**, 12892-12898.

[16] P.J. Ross: 'Taguchi Techniques for Quality Engineering', 2nd edn; 1996, United States, McGraw-Hill.

[17] R.K. Roy: 'A premier on the Taguchi Method'; 1990, New York, Van Nostrand Reinhold.

[18] R. French and S. Czernik: 'Catalytic pyrolysis of biomass for biofuels production', *Fuel Processing Technology*, 2010, **91**, 25-32.

[19] H.J. Park, J.K. Jeon, D.J. Suh, Y.W. Suh, H.S. Heo, Y.K. Park: 'Catalytic Vapor Cracking for Improvement of Bio-oil Quality', *Catal Surv Asia*, 2011, **15**, 161-180.

[20] Z. Du, X. Ma, Y. Li, P. Chen, Y. Liu, X. Lin, H. Lei, R. Ruan: 'Production of aromatic hydrocarbons by catalytic pyrolysis of microalgae with zeolites: Catalyst screening in a pyroprobe', *Bioresource Technology*, 2013, http://dx.doi.org/10.1016/j.biortech.2013.04.053

[21] S. Yorgun and Y.E. Şimşek: 'Catalytic pyrolysis of Miscanthus x giganteus over activated alumina', *Bioresource Technology*, 2008, **99**, 8095-8100.

[22] N. Thanh-An, K. Jinsoo, K. Sun Kuk, K. Seung-Soo: 'Pyrolysis of soybean oil with H-ZSM5 (Proton-exchange of Zeolite Socony Mobil #5) and MCM41 (Mobil Composition of Matter No. 41) catalysts in a fixed-bed reactor', *Energy*, 2010, **35**, 2723-2728.

[23] L. Tsung-Ying and K. Chun-Pao: 'Study of products yield of bagasse and sawdust via slow pyrolysis and iron-catalyze', *Journal of Analytical and Applied Pyrolysis*, 2012, **96**, 203-209.

[24] E.F. Iliopoulou, S.D. Stefanidis, K.G. Kalogiannis, A. Delimitis, A.A. Lappas, K.S. Triantafyllidis: 'Catalytic upgrading of biomass pyrolysis vapors using transition metal-modified ZSM-5 zeolite', *Applied Catalysis B: Environmental*, 2012, **127**, 281-290.

[25] D.J. Mihalcik, C.A. Mullen, A.A. Boateng: 'Screening acidic zeolites for catalytic fast pyrolysis of biomass and its components', *Journal of Analytical and Applied Pyrolysis*, 2011, **92**, 224-232.

[26] A.Aho, N. Kumar, A.V. Lashkul, K. Eränen, M. Ziolek, P. Decyk, T. Salmi, B. Holmbom, M. Hupa, D.Yu. Murzin: 'Catalytic upgrading of woody biomass derived pyrolysis vapours over iron modified zeolites in a dual-fluidized bed reactor', *Fuel*, 2010, **89**, 1992-2000.

[27] E. Butler, G. Devlin, D. Meier, K. McDonnell: 'A review of recent laboratory research and commercial developments in fast pyrolysis and upgrading', *Renewable and Sustainable Energy Reviews*, 2011, **15**, 4171-4186.

[28] F. Sulaiman and N. Abdullah: 'Optimum conditions for maximizing pyrolysis liquids of oil palm empty fruit bunches', *Energy*, 2011, **36**, 2352-2359.

[29] N. Abdullah and H. Gerhauser: 'Bio-oil derived from empty fruit bunches', *Fuel*, 2008, **87**, 2606-2613.

[30] N. Abdullah, H. Gerhauser, F. Sulaiman: 'Fast pyrolysis of empty fruit bunches', *Fuel*, 2010, **89**, 2166-2169.

[31] A.V. Bridgwater, D. Meier, D. Radlein: 'An overview of fast pyrolysis of biomass', *Organic Geochemistry*, 1999, **30**, 1479-1493.

[32] F. Broust: 'Conversion of solid biomass to liquid fuels: Bio-oil Production and Utilization'; 2009, available at http://redenacionaldecombustao.org/escoladecombustao/arquivos/EDC2009/palestras/palestra_bio_oleo_francois_broust.pdf (accessed 22 February 2013).

[33] M. Misson, R. Haron, M.F.A. Kamaroddin, N.A.S. Amin: 'Pretreatment of empty palm fruit bunch for production of chemicals via catalytic pyrolysis', *Bioresource Technology*, 2009, **100**, 2867-2873.